

## **Effect of experimental uncertainties on the calculation of the peeling-ballooning stability boundary**

A. Burckhart<sup>1</sup>, M. Dunne<sup>2</sup>, E. Wolfrum<sup>1</sup>, R. Fischer<sup>1</sup>, S. K. Rathgeber<sup>1</sup>, ASDEX Upgrade Team

<sup>1</sup> *Max Planck Institut für Plasmaphysik, Boltzmannstr. 2, D-85748 Garching, Germany*

<sup>2</sup> *Department of Physics, University College Cork, Association Euratom-DCU, Cork, Ireland*

Stability calculations using ideal MHD codes, such as MISHKA [1] in the framework of the ILSA package [2], are frequently used to determine the peeling-ballooning stability boundaries for type-I ELMy H-mode plasmas. Generally, a reference equilibrium, synthetic or experimental, is tested against peeling-ballooning stability and then modified in normalised edge pressure gradient  $\alpha$  and toroidal current density  $j_{tor}$  to scan the stability boundary. However, even small changes in the input data can have an influence on the results of the stability calculations. It is therefore important to investigate the extent of potential changes in the stability boundary due to uncertainties in the measured data. The main focus of this work is to determine the impact of different inputs on the stability calculations.

To calculate a full plasma equilibrium, the free boundary Grad-Shafranov solver CLISTE [3] uses the signals from over 60 normal and tangential measurements of the poloidal magnetic field. Optional inputs that improve the accuracy of the final equilibrium include the poloidal scrape off layer currents [4], motional Stark effect data and the radial profile of the total plasma pressure  $p$ , including the fast ion contribution. In practice, the kinetic constraints are restricted to the plasma edge, which is very well diagnosed and where the role of the fast ions is negligible. Recent findings show that the CLISTE equilibrium solver produces very accurate current density profiles when kinetic profiles and scrape off layer currents are used as constraints [5].

In this work, the pressure data was generated from the electron density  $n_e$  and temperature  $T_e$  profiles, which were calculated using the integrated data analysis (IDA) method. IDA combines the data from the DCN interferometer, the edge measurements from the Li-beam and the radiation temperature from ECE to calculate  $n_e$  and  $T_e$  via forward modeling [6]. The approximation  $T_i = T_e$  was used as no highly resolved edge charge exchange recombination spectroscopy (CXRS) data was available for the discharges covered in this work. The validity of this approximation has been shown for a similar discharge in reference [7]. The magnetic signals and the SOL currents are measured routinely at ASDEX Upgrade (AUG), but no MSE data was available. All the aforementioned data was ELM-synchronised using the method described in reference [8].

The type-I ELMy H-mode AUG discharge #23418 has already been studied extensively [8]. It has been shown that it features two distinct ELM frequencies, one around 80Hz and the other around 120Hz. In the fast ELM cycles the maximal pressure gradient  $\nabla p$  reached a limit after which the ELM immediately occurred. In the slow ELM cycles  $\nabla p$  reaches the same limit, but the gradient stayed at this value for up to 7ms before the ELM crash occurred (see Fig. 1, left). It has also been shown that current diffusion is too fast for a delayed bootstrap current to play a role as a delayed ELM trigger. In the following, the stability of three separate equilibria calculated with CLISTE will be assessed. To calculate a stability diagram, the equilibria were modified in  $p'$  and  $j_{tor}$  independently using the so-called j-alpha workflow included in the HELENA package [9]. In this work, 11 values of  $j_{tor}$  and  $p'$  were used. For each of these 121 grid points the ideal MHD stability code ILSA calculates the growth rate and mode structure of

different toroidal mode numbers  $n$ . The non-modified equilibrium that corresponds to the actual measurements will be referred to as the operational point and marked by a cross on the figures.

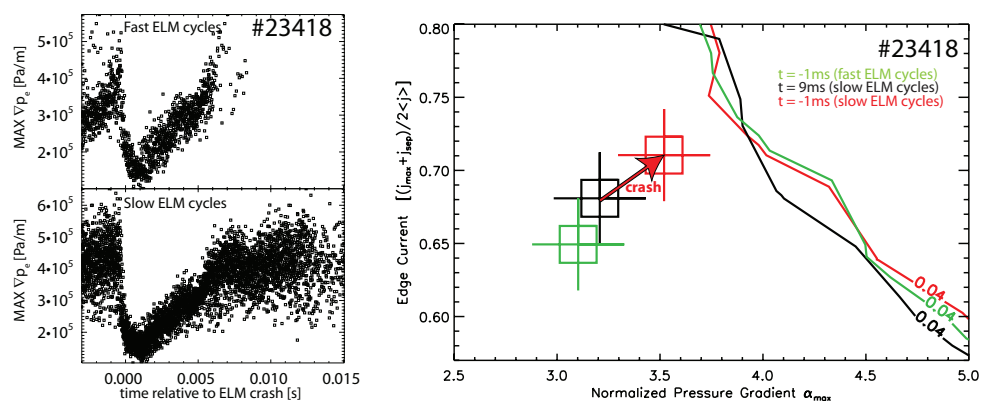


Figure 1: Maximal pressure gradient (left) and stability diagram (right) of discharge #23418

Figure 1 also shows the result of the stability analysis for discharge #23418. The crosses correspond to the operational points in the  $j - \alpha$  grid. The lines indicate the region where the plasma becomes marginally unstable (see also [10]). The red data mark the stability of the plasma calculated just before the ELM crash in the slow cycles, green in the fast cycles and black corresponds to an equilibrium in the slow cycles where the pedestal had already fully recovered, but the ELM crash was still about 6ms away. The differences between the stability properties are rather subtle. In the last  $\sim 6\text{ms}$  of the slow ELM cycle,  $\alpha$  increased by less than 10%, which is well within the experimental errors and the scatter of the data (see Fig. 1, left, and reference [8]). The stability boundary itself seems to be invariant, since all three cases mostly overlap. To assess whether the boundaries are really robust or if experimental errors play a significant role, different sensitivity studies have been performed.

The two main uncertainties in the experimental measurements are the ion temperature, which was assumed to be equal to  $T_e$ , and the electron temperature gradient. Previous IDA applied 'classical' ECE analysis, which identified the electron temperature with the radiation temperature ( $T_{\text{rad}}$ ) at the cold resonance position of the measured frequency. Since this approach is not valid in optically thin plasma regions, previous IDA omitted these data and extrapolated  $T_e$  into the SOL. However, close to steep gradients  $T_e$  can also differ from  $T_{\text{rad}}$  in an optically thick plasma. Furthermore, the extrapolated  $T_e$  is under-determined. Therefore, IDA has recently been extended by electron cyclotron forward modelling (ECFM) which applies first principle physics to achieve reliable electron temperature profiles also in the edge gradient region [11, 12]. The enhanced IDA analysis will simply be referred to as ECFM and the previous ECE analysis as classical IDA. The effect of the corrected  $T_e$  gradients on the stability was assessed for #23417, a discharge very similar to #23418, but for which ECFM results were available.

The four stability diagrams in figure 2 represent the equilibria 3ms before the ELM crash in discharge #23417 for the fast (pedestal still recovering, top) and slow (fully recovered pedestal, bottom) ELM cycles, using the classical IDA analysis (left) and ECFM (right). It can be seen that in the slow ELM cycles the classical IDA profiles lead to a pressure gradient and edge current density that are 20% lower than the stability boundary, whereas when using the ECFM method the operational point is in the marginally unstable region. Note that since the assumption  $T_i = T_e$  was used, and recent highly resolved edge CXRS measurements suggest that  $\nabla T_i$  is

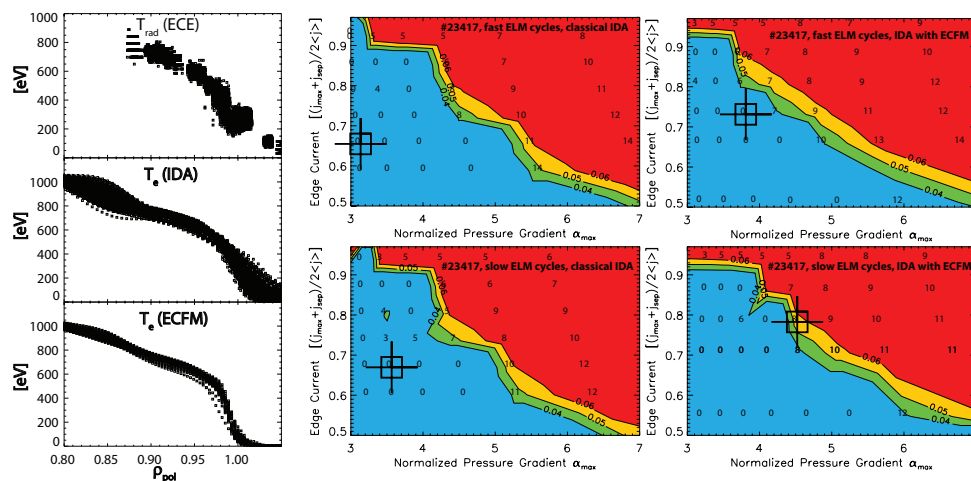


Figure 2:  $T_e$  profiles (left) and stability diagrams (right) of AUG #23417

slightly lower than  $\nabla T_e$ , the correct operational point might be just outside of the unstable region. In the equilibrium 3ms before a fast ELM crash, the operational point is not quite on the stability boundary, which is to be expected since the profiles have not yet fully recovered. In this case, the difference between the equilibrium obtained using ECFM and the one generated with classical IDA is also very strong. Nevertheless, the position of the stability boundary itself barely changes between the four cases. This suggests that the stability calculations are rather robust against errors in the kinetic data used for computing the input equilibrium. However, accurate kinetic data and current density profile are needed for identifying the exact position of the operational point, which determines whether the plasma is unstable or not.

A second potential systematic error is the location of the steep gradient region in relation to the equilibrium separatrix location. In order to assess this, the kinetic profiles were shifted by  $\pm 5$ mm before the CLISTE equilibrium was solved. The resulting perturbed equilibria were then analysed with ILSA.

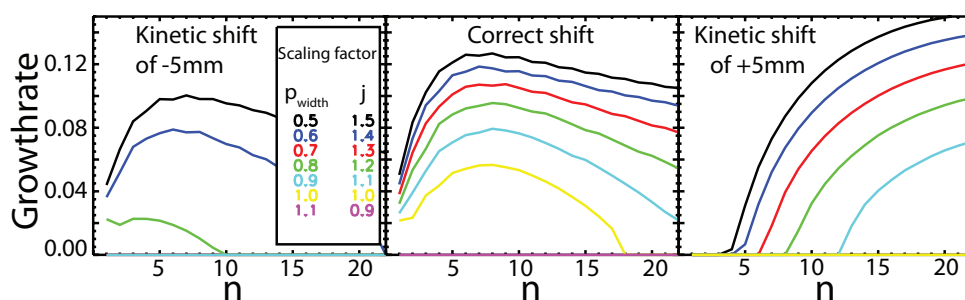


Figure 3: Toroidal mode spectra for three different shifts between kinetic and magnetic data

A very strong dependence of the toroidal mode spectrum can be seen in figure 3. The higher growthrate for an outward shift of the pressure profile and current density is to be expected, but it can also be seen that the toroidal mode numbers increase for a strong outwards shift. Therefore, much care has to be taken when aligning the kinetic data. A poor alignment can be detected via carefully monitoring the residuals from CLISTE.

Another source of error can be the truncation parameter  $\Psi_b$ . The codes HELENA and ILSA use the straight field line coordinate system and can, therefore, not deal with a separatrix. The

plasma must be cut off at a normalised flux (usually around 0.995) in order to limit the safety factor  $q$  at the edge. It has been shown that the presence of a separatrix has a stabilising effect on the peeling-ballooning modes and that the equilibrium becomes more unstable when more flux is cut off [13]. To assess the impact of  $\Psi_b$  on the stability in this case, two equilibria of discharge #23417 using ECFM in the slow ELM cycles were used for a sensitivity study. The first equilibrium corresponds to the non-modified operational point, in the second one the edge current was increased and the pedestal width decreased by 30%. Figure 4 shows the growth rates of the different toroidal mode numbers  $n$  for those two cases.  $\Psi_b$  was varied between 0.980 and 0.999. The oscillations of the extreme cases 0.980 and 0.999 with steepened profiles show that they are numerically unstable. The cases that seem to be missing on the plot have a zero growth rate for all mode numbers.

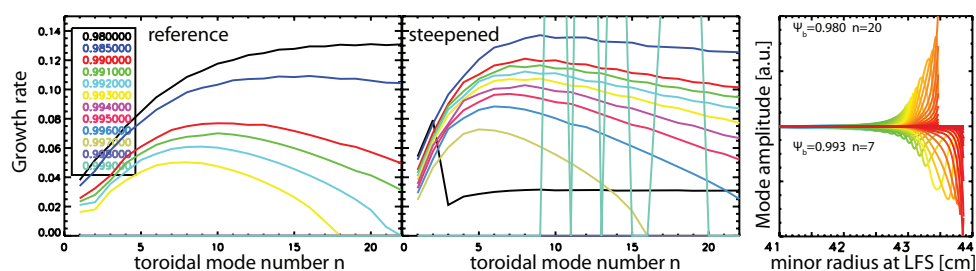


Figure 4: Left: toroidal mode spectrum of two equilibria for different  $\Psi_b$ . Right: poloidal mode structure for two  $\Psi_b$  in the reference case

Figure 4 shows that in both cases the truncation parameter has a significant impact on the calculated stability of the different modes. The mode number decreases with higher  $\Psi_b$ . The non-modified equilibrium (left) can range from completely stable (cut off close to the separatrix) to very unstable ( $\Psi_b \approx 0.985$ ). The poloidal mode structure of the fastest growing toroidal mode in the black and the yellow curve are shown on the right hand side of figure 4. The sign and absolute amplitude are arbitrary, but  $n=20$  has a lower width than  $n=7$ . Since more flux has been cut off, the actual extent in the plasma is similar.

In conclusion, the stability boundary is rather robust against errors in the data used to generate the equilibrium. Thanks to recent analysis improvements the operational point can be determined much more accurately. A misalignment of a few millimetres of the position of the pressure input relative to the magnetic measurements has a large impact on the stability calculations. The truncation parameter  $\Psi_b$  also has a very strong influence on the stability calculations. A correct and robust criterion should be found for the choice of  $\Psi_b$ .

## References

- [1] A. Mikhailovskii *et al*, Plasma Phys. Rep., **23**, 844 (1997)
- [2] C. Konz *et al*, 38th European Conf. on Plasma Physics (Strasbourg), O2.103 (2011)
- [3] P.J. Mc Carthy, Plasma Physics and Controlled Fusion, **54**, 015010 (2012)
- [4] A. Kallenbach *et al*, Journal of Nuclear Materials **293** 639-643 (2001)
- [5] M. Dunne *et al*, 39th European Conf. on Plasma Physics (Stockholm), O4.110 (2012)
- [6] R. Fischer *et al*, Fusion Science and Technology **58** 675-684 (2010)
- [7] E. Wolfrum *et al*, Plasma Physics and Controlled Fusion **51** 124057 (2009)
- [8] A. Burckhart *et al*, Plasma Physics and Controlled Fusion, **52**, 10 (2010)
- [9] F. Osmanlic *et al*, to be submitted (2012)
- [10] C. F. Maggi *et al*, Nuclear Fusion **50** 025023 (2010)
- [11] S. K. Rathgeber *et al*, submitted to Plasma Physics and Controlled Fusion (2012)
- [12] S. K. Rathgeber *et al*, 39th European Conf. on Plasma Physics (Stockholm), P5.059 (2012)
- [13] G. T. A. Huysmans, Plasma Physics and Controlled Fusion **47** 12 (2005)